We are IntechOpen,
the world's leading publisher of
Open Access books
Built by scientists, for scientists

6,900
Open access books available

185,000
International authors and editors

200M
Downloads

Our authors are among the

154
Countries delivered to

TOP 1%
most cited scientists

12.2%
Contributors from top 500 universities

CLARIVATE ANALYTICS
BOOK CITATION INDEX
INDEXED

WEB OF SCIENCE™

Selection of our books indexed in the Book Citation Index
in Web of Science™ Core Collection (BKCI)

Interested in publishing with us?
Contact book.department@intechopen.com

Numbers displayed above are based on latest data collected.
For more information visit www.intechopen.com

Measurement Methods and Extraction Techniques to Obtain the Dielectric Properties of Materials

Turgut Ozturk and Muhammet Tahir Güneşer

Additional information is available at the end of the chapter

Abstract

Material characterization plays an important role in many applications that are called as security, military, communication, bioengineering, medical treatment, food industry, and material processing, since it is useful to identify other properties such as stress-strain relation, bio content, moisture content, materials density, etc. Therefore, the dielectric properties of materials should be achieved with high accuracy using appropriate measurement techniques and extraction techniques. There are many measurement methods to obtain the dielectric properties of materials, which can be divided into two categories: up conversion and down conversion methods. A microwave measurement method can be called as frequency up conversion, while THz time-domain spectroscopy (THz-TDS) system is a frequency down conversion method. The selection of more convenient measurement method depends on some parameters such as frequency range, material phase, and temperature. In this chapter, the measurement methods and extraction techniques will be discussed, and alternative ways will be presented with experimental and simulation results.

Keywords: complex permittivity, dielectric materials, free space measurement, material characterization, Newton-Raphson, terahertz radiation, THz, time-domain spectroscopy

1. Introduction

The complex permittivity of materials is independent of available measurement methods. This parameter has an important place for material characterization in electrical and electronics engineering. It can be used to recognize the interaction between a material and an electromagnetic radiation. In many applications, knowing of some parameters of the material, which is

cheaper than trial-error method, facilitates the work of engineers. Therefore, materials characterization and measurement methods are increasingly gaining importance at mm waves and THz frequency ranges. For instance, the knowledge of behavior of materials in these frequency ranges is essential to design and produce new equipment for astronomy or remote sensing applications.

It is possible to divide the measurement methods into two categories as up and down frequency conversion methods. In this context, the optical measurement methods can be called as a down-conversion method, and its aim is to decrease the frequency from 10^{14} Hz to 10^{12} or 10^{11} Hz. The well-known down conversion (optical) measurement method is Terahertz time-domain spectroscopy (THz-TDS). Usually, a femtosecond laser source is used to excite receiver and transmitter photoconductive antennas. Millimeter wave or microwave measurement methods can be called as an up-conversion method because of using frequency extenders to obtain the hundreds of GHz, and the purpose of it is to increase the frequency from 10^{10} Hz to 10^{11} Hz. The most preferred method is free space measurement (FSM) method in this category. Generally, a sample is placed between two horn antennas, and the measurement process is controlled by a Vector Network Analyzer (VNA).

Many different extraction techniques were investigated to obtain the high accuracy for the dielectric parameters, and they are usually divided into two groups as analytical (Nicolson-Ross-Weir [NRW] or NIST Iterative) and numerical (Newton-Raphson or Genetic Algorithm) techniques. In addition, the artificial intelligence (AI) methods are used to extract the dielectric properties to provide support the numerical techniques. To obtain the dielectric constant, numerical techniques are preferred to eliminate the associated error between sample thickness and frequency. However, there is an initial value problem in this approach. Therefore, both analytical and numerical techniques should be tried to achieve the most accurate result.

2. Dielectric properties of materials for material characterization

The dielectric properties of a material are related to other properties of that material. Humidity and temperature in the environment, the density of the material, its structure, the amount of water in it, and the porosity can change the dielectric properties of the material for the frequencies of microwave, millimeter wave, and THz [1, 2]. Besides, the thickness of the material, the chemical composition, and especially, the permanent dipole moment also affect the dielectric properties of a material. In addition, the effects of electromagnetic interference are needed to take in the account considering the environmental conditions [3].

The complex permittivity, which is an internal characteristic of material independent of the measurement technique, is accepted an important value of material characterization for electrical engineering [4]. Dielectric constant and loss tangent, which are electrical characteristics of material, play an important role in the propagation of the electromagnetic energy in the insulating medium. Therefore, the permittivity determines the propagation speed of the electromagnetic wave and the amount of stored energy on the material.

The dielectric properties of a material consist of relative dielectric constant (ε_r) and magnetic permeability constant (μ_r), which are represented by the equations $\varepsilon = \varepsilon_0 \varepsilon_r$ and $\mu = \mu_0 \mu_r$. $\varepsilon_0 = 8.52x10^{-12}$ (F/m) and $\mu_0 = 4\pi x10^{-7}$ (H/m) are the values of permittivity and permeability of the cavity, respectively [5]. When an electromagnetic wave is applied to a material, the interaction of the material is expressed by two basic functions: permittivity and permeability. The complex permittivity consists of real and imaginary parts as seen on Eq. 1 [6]:

$$\varepsilon = \varepsilon_r - j\varepsilon_i \tag{1}$$

where ε_r is real, which represents stored electric field energy on the material, and ε_i is imaginary, which is amount of electric field loss. In case $j = -1$ on Eq. 1, the rate of imaginary $(\varepsilon_i/\varepsilon'')$ over real $(\varepsilon_r/\varepsilon')$ is called as loss tangent seen on Eq. 2.

$$\tan(\delta) = \varepsilon_i/\varepsilon_r \tag{2}$$

The imaginary part is also correlated with electrical conductivity (σ) as seen on $\varepsilon_i = \sigma/\varepsilon_0\omega$, where ω is angular frequency. Orthogonal axis representation of real and imaginary parts of complex permittivity is seen in **Figure 1**.

The propagation of the electromagnetic wave in a material depends on its permittivity and permeability. When the impedance of the waveguide in the material (Z) is lower than free space impedance (Z_0), impedance mismatch occurs. During the propagation through the material, some of the energy are transmitted, and some are also reflected. In other words, material and electromagnetic wave interaction occur in three ways: reflection, absorption, and transmission [5].

Propagation speed of the waveguide through the material (v_m) is lower than speed of light (c). Since the frequency (f) is constant, the wavelength (λ_m) is seen shorter than free space
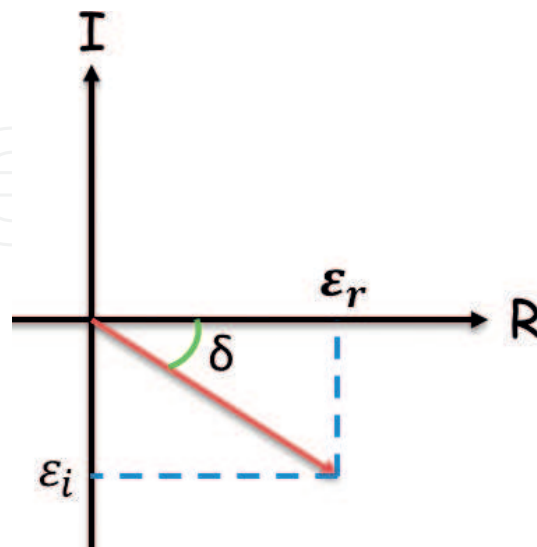

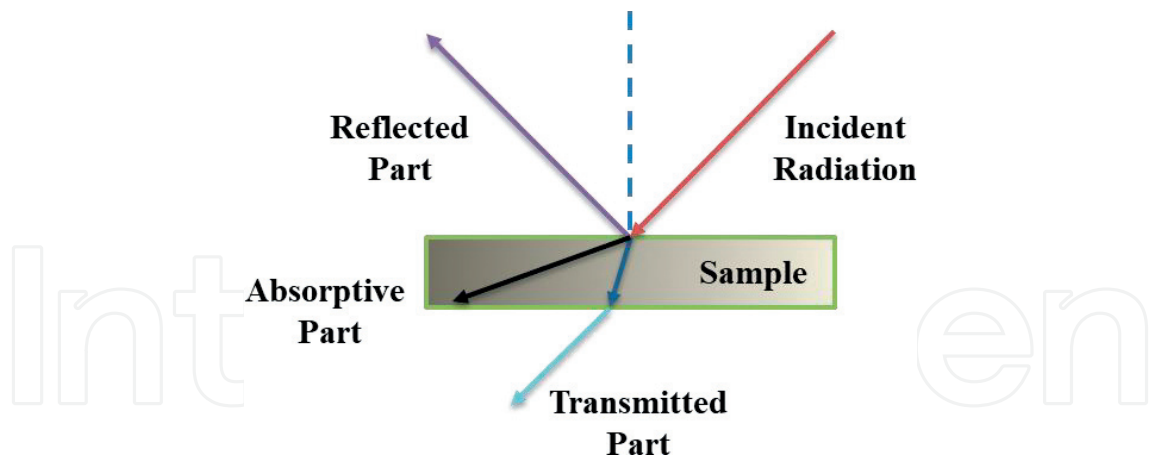**Figure 1.** Representation of complex permittivity.

Figure 2. Interaction of electromagnetic wave with material.

wavelength (λ_0). Transition and propagation of a waveguide to a single layer material are seen in **Figure 2** [7].

In an electromagnetic field, propagation paisley expression of a transverse electromagnetic (TEM) plane wave on $+z$ direction is displayed as $E(z, \omega) = E_0 e^{-\gamma z}$, where the angular frequency is calculated as $\omega = 2\pi f$ and γ represents the propagation of the waveguide [8].

3. Measurement methods

Two different measurements, which are optic and microwave methods, are used in material characterization processes of THz frequency range. THz waves have unique properties such as being able to pass through some materials, which are not so permeable for other parts of the electromagnetic spectrum, or reflecting from some materials close to 100%, being harmless compared to X-rays, and having the ability to distinguish between different materials. The change of wavelength and frequency related to the THz gap is shown in **Figure 3**.

The time-domain spectroscopy (TDS) system, which is created in parallel with technological developments, is still expensive due to its most important component femtosecond lasers, and
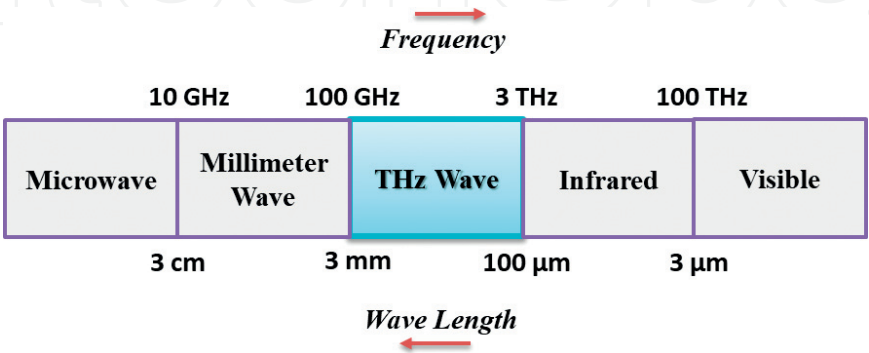

Figure 3. Showing a part of electromagnetic spectrum.

it is generally not reliable and stable enough for long-term industrial use. To solve the problems of laser source in TDS system, Multimode Laser Diode (MLD), which is smaller, simpler, cheaper, stable, and commercially available, is used alternatively. Although MLD-TDS is weaker than traditional THz-TDS in terms of radiant power, radiation efficiency, and spectrum width, it has been shown in some studies that these points can be improved [9–11].

The microwave measurement systems including frequency up conversion methods are actively used in material characterization processes in THz frequency domain as an alternative to conventional TDS systems. However, only one of these methods cannot be used effectively on whole frequency band to measure the dielectric properties of the material. Moreover, several difficulties were seen in measuring lossy and low-loss materials with high accuracy. Therefore, different methods are needed for each band and material loss [6, 12]. The factors, such as measured frequency range, the expected value of the permittivity, required measurement accuracy, properties of the material (homogeneous, isotropic), and form of the material (solid, liquid, and gas), must be taken into consideration during the method determination. In addition, conditions such as sample size constraints, temperature, contact/noncontact measurement, and destructive/nondestructive measurement must be considered [12, 13].

Although the analyzed material differs according to where they are applied, the basic process is to completely determine the dielectric properties. In this framework, researches have been carried out on the analysis of many kinds of materials, and the results are shared. Some researches attempted to determine the effects of ambient conditions, which are created for the preservation of foods and preservation of freshness for a long time in food industry, on the material by the change in the permittivity [14, 15]. Successful studies have been conducted to examine the effect of changes in humidity on the freshness of the food [16, 17].

There is no single measurement technique for all conditions in the direction of these items. For this reason, a more precise measurement can be performed after determining which measurement method is suitable. If desired frequency range is high, free space measurement (FSM) method is the most suitable one by considering current technology.

3.1. Free space measurement method

Since the fact that it is aimed to work in THz frequency range, free space measurement method that is one of microwave measurement methods is at the foreground due to many advantages. FSM method especially offers the possibility of especially nondestructive and noncontact measurements, characterization of solid-liquid-powder materials, and measuring solid materials except very small ones.

Generally, measurement techniques, which are used in microwave and millimeter wave frequency regions, can be classified into two groups as resonant and nonresonant methods. Materials can be analyzed at single or discrete frequencies with resonant method. But with the nonresonant method, the analysis of materials can be pursued over a wide frequency band [6]. Recently, the most preferred methods of analysis for frequency bands above 1 GHz are listed as waveguide, coaxial probe, resonant cavity, and free-ambient measurement method [5, 18].

Nonresonant methods are used to determine electrical and magnetic properties over a wide frequency range, but resonant methods are better suited for calculating only single frequency [19]. Commonly used methods, which are including basic functions that must be included in a measurement method, are compared in **Table 1**, where ND is Nondestructive, S is Solid, L is Liquid, and G is Gas [5, 6]. Some of these techniques are more suitable for solid materials and others for liquids. It is also important that the analysis method is simple, as well as cheap [20].

FSM method has better dynamic capacity and spectral resolution than other methods [21]. However, FSM method could not be widening unless development of measuring devices for last decade [22]. Thus, measurement of the complex permittivity is possible over a wide frequency range by means of advanced measuring equipment and the FSM method accurately [23]. The FSM method consists of two antennas connected to a Vector Network Analyzer (VNA), and between the two antennas a sample holder in which the material to be measured is placed as shown in **Figure 4** [9, 24].

The quartz plates are not required in measurement setup if measurements are taken for solids like Teflon or glass. Because sagging of solid materials can be neglected when the sample

	FSM	Waveguide	Coaxial probe
Dielectric features	ε_r-μ_r	ε_r-μ_r	ε_r
S-parameter	S_{11}-S_{21}	S_{11}-S_{21}	S_{11}
Frequency band	Wide	Discrete	Wide
Dimension	Large	Medium	Little
Testing procedure	ND	Destructive	ND
Sample preparation	Easy	Hard	Easy
Form of material	S-L-G	S	S-L
Monitoring	Very easy	Hard	Easy

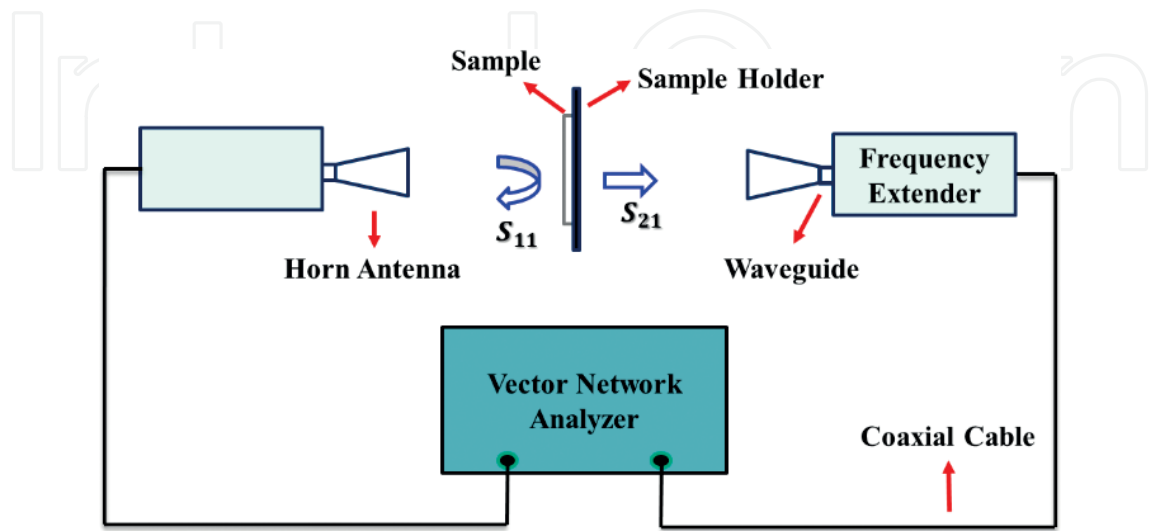**Table 1.** Comparison of commonly used microwave measurement methods.

Figure 4. Schematic representation of FSM method.

holder is properly placed [7]. VNA is standard equipment of microwave and millimeter wave measurement systems for simultaneous measurement of S-parameters, which are used for calculating dielectric features of materials [22].

3.1.1. Features of FSM method

The accuracy of the measurements is increased by a high time domain solution with FSM method, even requiring a simple test setup for installation [25]. FSM method provides to measure S parameters under the conditions as contactless, nondestructive, and high temperature with wide frequency range and different substance forms and especially for nonhomogeneous materials. It is preferred to coaxial and waveguide measurement methods, since it does not need sample preparation [18, 26]. Another disadvantage of waveguide method is seen as leakage around the sample and limitation of sizing sample [27]. Moreover, waveguide and coaxial measurement methods both need for proper preparation of the sample. This requirement causes limitation of measurement accuracy for nonprocessable substances [28].

Spot focus can be achieved using lenses that will minimize the diffraction effect for high accuracy measurements [23, 26]. The antenna gain can also be increased, thanks to lenses that align the beam and reduce the diameter [29]. Additionally, the measurement errors can be reduced by TRL calibrations and VNA gating techniques [27]. Selecting the size of the sample larger also provides reduction of the diffraction effect. But larger specimens cause sagging problem especially nonrigids [7]. Even when the optimum thickness is achieved at the sample, another measurement error can be seen because the phase that is on the sample may not be planar. To prevent this, the effect of thickness must be taken into account in order to match the center of the sample with the point of the thinnest beam, which is aligned through the lens [30].

3.1.2. Measurement with FSM method

A software was developed for analysis and defining the material. Therefore, firstly, the materials, which had been analyzed in microwave and millimeter wave frequency bands, were measured and compared with other studies in the literature to confirm and ensure the accuracy of the developed software. The calculation techniques were optimized for the analysis of the data obtained by the FSM method, which constitutes a significant part of the study. Most appropriate algorithm was determined to use the output of characterizations for recognition of materials, and the results were proved.

Several experiment setups of FSM method were used to show the interaction of the electromagnetic waveguide with the material at different angles for determination of the dielectric properties of a material. In this system, the signals, which are reflected and transmitted from the sample surface, are collected as shown in **Figure 4**. FSM method is preferred for all measurements over than 75 GHz. At other frequencies, the antennas and distances between them were changed to keep the system as reliable. In order to be able to measure in the frequency range of 75–325 GHz by FSM method, four different experimental setups were required. For this reason, antenna structures (WR10, WR8.0, WR5.1, and WR3.4) were changed, and measurements were taken in four different stages up to 325 GHz. To be able to measure up to 500 GHz (between 325 and 500 GHz), WR2.2 antenna structure must be used in the fifth stage.

Measurements were made in the 75–325 GHz frequency range without using a parabolic mirror. The results of analyzed materials (Paper, Ultralam, PVC, Glass, Teflon, L1000HF, Rexolite, and RO3003) are seen in **Figure 5**. Newton-Raphson technique was used in the calculations. Lowest and highest values were entered for prediction of the algorithm instead of classic initial value assignment. Only specified (S_{21}) parameter of the materials is used for determining the complex permittivity.

For the first time, an analysis of the materials given in **Figure 5** has been made and shared in this frequency range. Due to the different measurement methods and using of different calculation techniques, little negligible differences can be obtained in the results. As the frequency band expands, the change in the dielectric constant values is not constant. For this reason, the thickness and dielectric constant values of each material are shown in **Table 2**. Ultralam, L1000HF, RO3003, and Rexolite materials measured different thicknesses as they are supplied from the manufacturer with different dimensions.
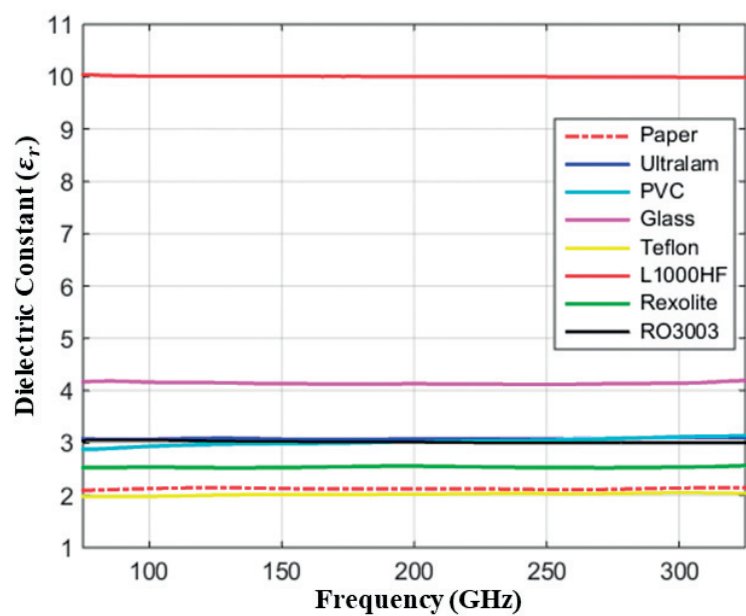

Figure 5. The dielectric constants of materials obtained by FSM method.

Material	Thickness (mm)	Dielectric constant
Paper	0.15	2.10–2.14
Ultralam	0.17	2.95–3.10
PVC	0.25	2.90–3.05
Glass	3	4.12–4.16
Teflon	4	1.98–2.05
L1000HF	3.20	9.95–10.05
Rexolite	12.85	2.52–2.55
RO3003	1.53	2.99–3.05

Table 2. Measurement of materials in W-band (75–110 GHz).

3.2. Multimode laser diode: time-domain spectroscopy (MLD-TDS) system

Various methods such as poorman's THz-TDS, Quasi-TDS (QTDS), and MLD-TDS are invented to obtain THz signal. In last two decades, the studies about multimode laser diode (MLD) that one of them can be grouped in three as THz pulse generation, sample analysis, and 2D imaging [10, 31–33]. Photoconductive antennas provide THz radiation by generating current ripple at pico-second time interval. To do this, a sudden fluctuation of the beam from the MLD is used [34, 35]. The idea of generating THz pulses from an MLD with this feature has been proposed by Hangyo. In his study, MLD-induced Photo-Conductive Antenna (PCA) is shown to be capable of producing THz pulses, and the THz pulse was measured with a bolometer that was sensitive to temperature change instead of antenna [33, 36]. In this first study, Hyodo and his colleagues used an experimental setup and added MLD instead of a dual-chip microchip laser as a beam source [36, 37]. In later researches, similar systems have been established, and obtaining THz pulses are aimed with different antenna structures. In addition, the dielectric constant and refractive index of the sample were measured to define the material [11, 34, 38].

3.2.1. Features of MLD for TDS system

Spectroscopy systems determine the response of the material to electromagnetic fields. THz-TDS system can be simply expressed in terms of production and detection of THz radiation in time domain. Two optical arms are seen in such systems in the same experimental setup as one for production and the other for detection. Ultra-fast lasers (UFL) are used as a beam source in this system. THz radiation is produced by one of the two branches of the incoming beam. THz waveform is obtained as a function of time, while the detection beam is scanned by interferometric steps. The first measurement of THz waveform is used as reference information. Spectroscopic information about the sample is obtained by examining the measurements of THz-TDS under the Fourier Transform (FD). In general, the time shift in main THz peak, the change on refractive index, and amplitude are related with power absorption of the sample [39].

MLD is proposed as an alternative cheaper and smaller beam source to design TDS systems, which are frequently used in material characterization and imaging processes [36]. The researches show that the signals obtained via MLD are like those obtained via the TDS one. THz pulse can be generated between the frequencies of 0.1–1 THz [10, 36].

PCAs are electrical components of MLD-THz spectroscopy system, and others are passive components. When the system is installed, first the passive components, then the electrical components are placed. The test setup consists of the generation and detection paths. The beam paths and system components of MLD-TDS are shown in **Figure 6**.

The working principle of the developed MLD measurement system is like the THz-TDS system. The light beam, from the MLD, is divided into two by the beam splitter. The beam, which follows the two paths known as generation and detection arms, is focused on the antennas by the objective lens. The signals emitted by the antennas are directed by parabolic mirrors. PCA, a device made of a semiconductor material, known changed the electrical conductivity when interacting with light, can convert infrared rays to THz. By exciting with
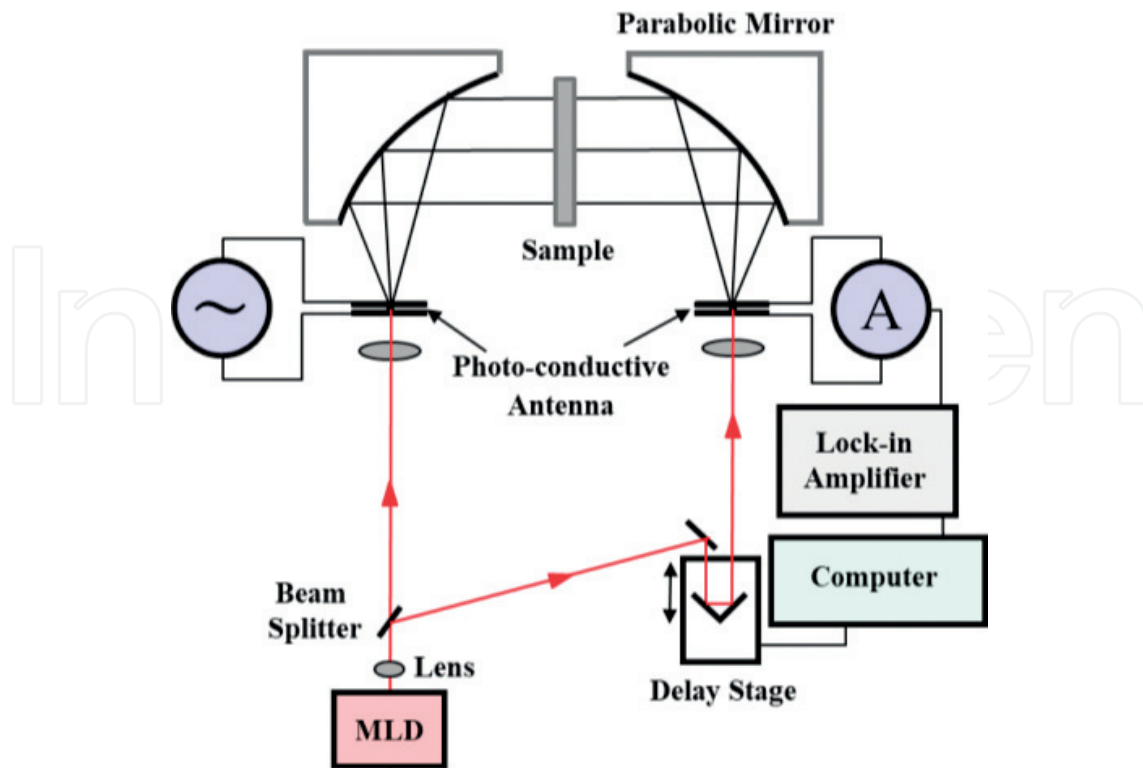
Figure 6. Schematic representation of MLD-TDS system.

laser beams focusing on the photoconductive antenna, the carriers are accelerated. Thus, the conductivity is increased and the photoaxis is created by a voltage signal from the function generator THz signal, radiating from the silicon lens face of the antenna, producing THz electric field. The relationship between the light intensity induced by the lock-in amplifier and the THz electric field is obtained as a function of the delay time. The delay time generated for the THz pulse is mechanically designed. Voltage/current values obtained from the locked amplifier are stored by LabVIEW software and plotted THz wave profile by time.

When previous researches are analyzed, only very low energy THz signals could be obtained. If the energy goes up, the nonlinear effect will decrease. However, this is an undesirable situation in MLD-TDS systems. Obtained signal should be at least 25 times of the noise. But the magnitude of obtained THz pulse by MLD is one hundredth or millionth of the magnitude of the pulsed system [15]. Therefore, the diameters of the parabolic mirrors should be large and positioned as close to the antenna as possible. The focal length of the parabolic mirror should be small, and the solid angle should be large to obtain higher signal. And of course, used antenna should be compatible with MLD-TDS systems.

3.2.2. Measurement with MLD-TDS system

The parabolic mirrors are used in the system for better collecting and aligning of generated THz signals, and the ambient conditions are most effective factors in weakening THz signal. If the focal points of the parabolic mirrors are less than 10 cm, the power of THz signal can be maintained. Since THz signals produced by MLD-TDS have very low amplitude values (Volt

or Ampere) than THz-TDS systems, the signal should align meticulously and the distance of the catheter should be short.

In the material characterization process with TDS systems, firstly, the refractive index should be calculated to determine the dielectric constant. Refractive index is given by amplitude difference between sampled and unsampled measurements in pico-seconds the shift of the THz signal. The waveform of obtained data, from w/o sample measurements of PVC sample, is seen in **Figure 7**. This spectroscopy system consists of MLD, driver, and cooler. Mostly, the softwares called Origin and Pkgraph are used for analysis. Origin was preferred for this study because of visual advantages of its interface.

Two different equations are used to calculate the refractive index depending on time and frequency. The refractive index can be obtained via Eq. 3, where Δt (s) is the shift of THz signal that is interacted with the sample. c and d represent speed of light (mm/s) and thickness of the material (mm), respectively.

$$n = \frac{c\Delta t}{2d} \tag{3}$$

$$n = \sqrt{\varepsilon_r \mu_r} \tag{4}$$

The complex permittivity (ε) of PVC was calculated by using Eq. 4 and expressed as shown in **Figure 8**. Signal degradation occurs after frequency of 0.6 THz on the measurements results obtained with MLD spectroscopy system. But signal quality is observed promising up to 0.8 THz for some material measurements. The measurement capability of the system is suitable up to about 1.2 THz, but the diagram of the signal is limited to 0.8 THz for more accurate material characterization.

Quality of THz signal obtained via MLD-TDS is not as good as ultra-short femtosecond laser source using TDS systems, but the measurement results of MLD-TDS are at least as successful
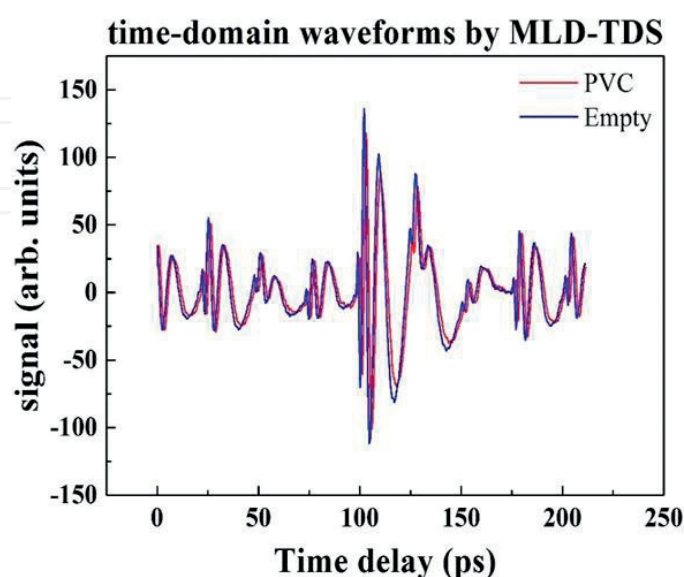

Figure 7. The measuring of PVC material by MLD-TDS system.
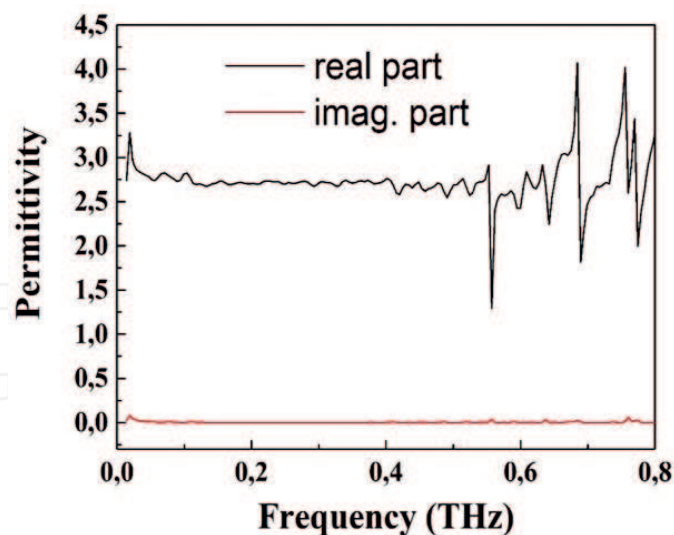
Figure 8. The complex permittivity of PVC sample.

as them. Researches on MLD-TDS systems are increasing because of being cheaper and more compact than THz-TDS. In this study, cheaper laser driver and cooler were used instead of conventional ones. Cooling is very important subject for MLD not to shift on mode spacing, which prevents THz signal generation, and if the limit current value to be applied to MLD is exceeded while supplying laser driver circuit, MLD will run like a standard LED emitting 808-nm laser beam.

3.3. Quasi-optical FSM method

The distance between the antennas should be kept within a certain range for generating planar wave while using FSM method. The distance between the antennas can be reduced by forming the planar waveguide at a shorter distance using the lens and parabolic mirrors. When parabolic mirrors are used to generate better THz signals and send aligning the center of the sample, the name of the system is revised as Quasi-Optical. Parabolic mirrors ensure more accurate data by focusing THz signal on the sample, and it enables to measure little-sized samples by FSM method [12]. Thus, sizing limitation problem of FSM method is already solved as seen in **Figure 9**.

Very precise adjustment is required to put parabolic mirrors since they align incoming beam. Normally, incoming beam is aligned by using infrared camera before PCA. Generated THz signal is directed to parabolic mirror, where it is aligned circular before sending next parabolic mirror. Aligning THz signal with the infrared camera is not so complicated since the wavelength of the beam is around 800 nm, but this is not so easy for FSM method. Repeat and repeat measurement may be needed while determining the position of the parabolic mirrors.

Before interpreting the results of measurements made with quasi-optical FSM method, some of mathematical approaches are needed to be clarified. When there is difficulty of generating THz signal with FSM method, highly likely expected error signals and unwanted situations should be eliminated. Some of signal correction techniques should be applied to correct the measured signals as seen below.
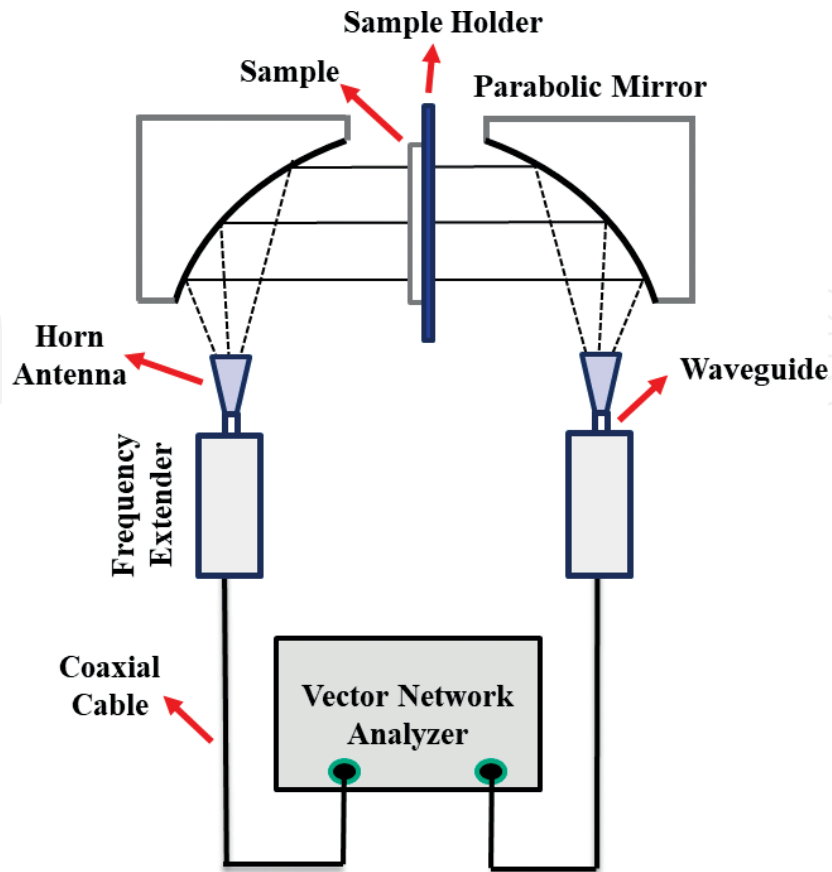
Figure 9. Schematic representation of quasi-optical FSM method.

Two different measurements are taken as with and without sample to perform the signal correction process, and the transmission (S_{21}) and the reflection (S_{11}) parameters are revised by considering these measurements as seen in Eq. 5 and 6, where m, c, a, and l represent material, correction, air (empty), thickness of the material, respectively, and β can be obtained via Eq. 7.

$$S_{21\_c} = \frac{S_{21\_m}}{S_{21\_a}e^{(j\beta l)}} \tag{5}$$

$$S_{11\_c} = \frac{S_{11\_m} - S_{11\_a}}{S_{21\_a}e^{(j\beta l)}} \tag{6}$$

$$\beta = 2\pi f\sqrt{\varepsilon_0 \mu_0} \tag{7}$$

However, some filtering methods may be needed if noise and error signals still exist. In this study, measurements were made at a frequency band of 140–500 GHz. Measurements of the material up to 325 GHz can be performed by using Quasi-optical FSM correctly even repeated a few times, when the calibration is done in a proper method. But for measurement at the band of 325–500 GHz, some of noise and error signals may still exist, even though signal correction

steps have been made. The Singular Spectrum Analysis (SSA) method should be applied to remove them after using Eq. 5 and 7 as seen in **Figure 10**.

Obtained revised transmission parameter (S_{21}) is used to calculate dielectric constant of the materials as shown in **Figure 11**. The high transmission amplitude parameter of the measured materials plays a facilitating role in the measurement. The dielectric constant of PMMA is seen about 2.6 (F/m) up to frequency of 325 GHz, but it decreases to 2.55 (F/m) for higher frequencies. For PVC, it is similar with about 2.9 (F/m) up to 325 GHz and 2.87 (F/m) at the band of 325–500 GHz.
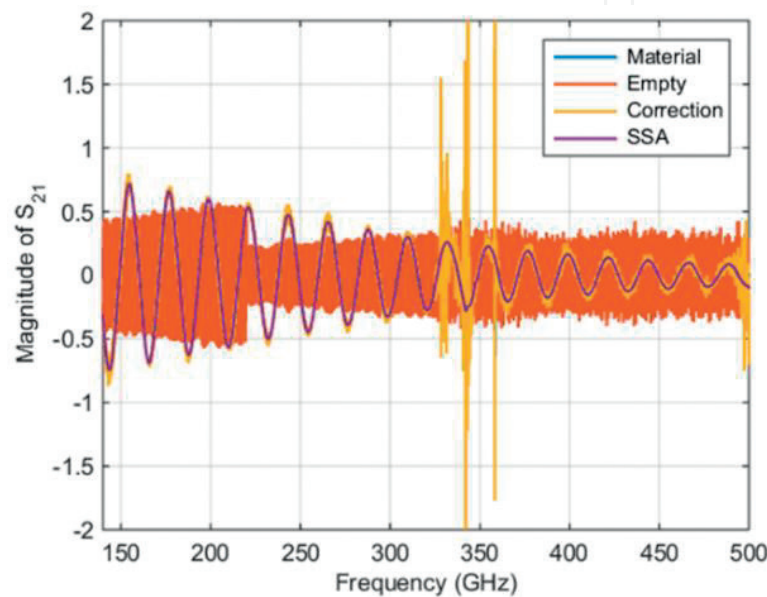

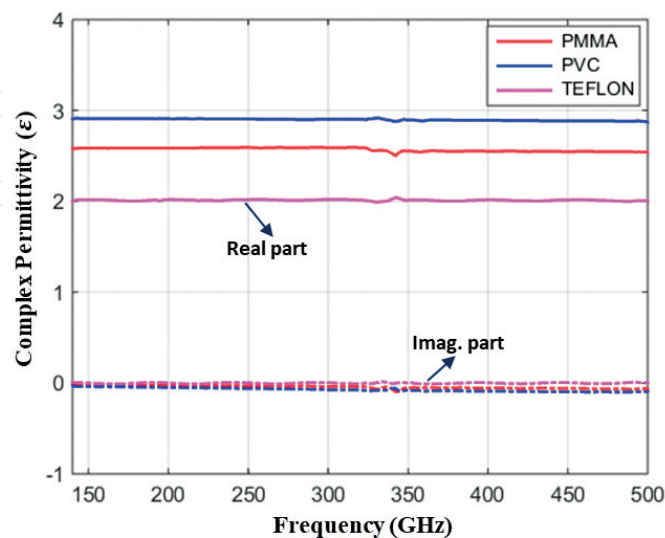**Figure 10.** Corrected signal of PVC sample.

Figure 11. The results of complex permittivity obtained via quasi-optical TDS.

4. Extraction techniques

Before measurements, the study includes the calibration, which is performed to collect the correct data, and the extraction, where the dielectric properties are determined after measurements. Different calibrating techniques were applied and compared in the studies [40–42]. The most basic extraction technique Nicolson-Ross-Weir (NRW) is widely used for extracting the dielectric properties [43, 44]. Numerical methods, such as Newton-Raphson (N-R), Genetic Algorithm (GA), and Root Finding Algorithm (RFA), are used as well beside of this analytical method. Artificial neural networks (ANN) algorithms, which can be learned by analysis of obtained data from calculation, are also used in estimating the complex permittivity [45–47].

The results, obtained from analyzed data by these extraction techniques, give an approximate value to the results of the mathematical theory. By optimizing these analytical and numerical techniques, the complex permittivity and refractive index of materials can be extracted with a smaller error rate and higher accuracy. To obtain more accurate results, the extraction techniques should be compared according to the above criteria and the most suitable one should be determined. Collected data by VNA are needed to purify from errors and noise. Indeed, the accuracy of the calibration is deteriorated especially while long-term measurements. Because of the difficulties of recalibration, filtering process is preferred.

4.1. Analytical and numerical extraction techniques

Basically, the complex permittivity and permeability of the materials are extracted by reflection (S_{21}) and/or transmission (S_{11}) parameters, which are called as scattering parameters [48]. In these processes, many techniques such as Nicholson-Ross-Weir (NRW), NIST, Root Find Algorithm (RFA), and Genetic Algorithm (GA) are used [45, 49]. The techniques used in the extraction process can be divided into two main categories as analytical and numerical. Details of most preferred NRW (analytical) and Newton-Raphson (numerical) extraction techniques are given in this study.

Analytical techniques generally require precise and explicit expression. For this reason, expressions are understandable and easy to use. However, in the NRW extraction technique, the equations become unstable and erroneous at a certain interval of the sample thickness. Therefore, analytical techniques are unstable for universal computational solutions [29, 50]. An iterative extraction method is proposed for dielectric materials to come from above resonances (to remove instantaneous peaks), when the sample thickness is greater than half the wavelength [51]. Unlike analytical techniques, numerical solution techniques, which are iterative methods, cover a wide range of algorithms. The biggest disadvantage of numerical extraction techniques is that it is necessary to estimate the value to be extracted before starting the extraction methods [29, 50].

4.2. Nicolson-Ross-Weir technique

The complex permittivity extraction technique, called NRW, was developed by Nicolson, Ross, and Weir [43, 44]. In this technique, transmission (T) and reflection (Γ) coefficients are extracted by using S-parameters. The NRW extraction technique is also the basis of other

techniques as it is relatively simple among other techniques [4]. In calculations, in FSM method, the cut-off wavelength (λ_c) is expressed as infinite, and the cut-off frequency (f_c) is expressed as a value very close to zero [5].

The dielectric constant of the material (ε_r) is calculated with the NRW technique by using S-parameters measured by the Vector Network Analyzer (VNA) and following the process steps [52]. Reflection coefficient (Γ) is expressed with Eq. 8, where $|\Gamma| < 1$ is required to find correct root. Unknown X is expressed by placing S-parameters as seen on Eq. 9, and transmission coefficient (T) can be calculated by Eq. 10. Also, the expression of a special equation of the inverse triangle (capital lambda) is calculated as seen on Eq. 11.

$$\Gamma = X \mp \sqrt{X^2 - 1} \tag{8}$$

$$X = \frac{S_{11}^2 - S_{21}^2 + 1}{2S_{11}} \tag{9}$$

$$T = \frac{S_{11} + S_{21} - \Gamma}{1 - \Gamma(S_{11} + S_{21})} \tag{10}$$

$$\frac{1}{\Lambda^2} = \left(\frac{j}{2\pi d} \ln(T) \right)^2 \tag{11}$$

λ_{og} can be calculated by using cut-off wavelength λ_c and free space wavelength λ_o as seen on Eq. 12, and the complex permittivity and permeability are calculated by Eq. 13 and 14, respectively. Eq. 8 and 9 are the basis for many analytical and numerical solutions.

$$\lambda_{og} = \frac{1}{\sqrt{\frac{1}{\lambda_0^2} - \frac{1}{\lambda_c^2}}} \tag{12}$$

$$\mu^* = \frac{\lambda_{og}}{\Lambda} \left(\frac{1 + \Gamma}{1 - \Gamma} \right) \tag{13}$$

$$\varepsilon^* = \frac{\lambda_o^2 \left(\frac{1}{\Lambda^2} + \frac{1}{\lambda_c^2} \right)}{\mu^*} \tag{14}$$

4.3. Newton-Raphson technique

Thanks to the iterative structure of the Newton-Raphson (N-R) technique, the best solution can be found. Only the transmission (S_{11}) or the reflection (S_{21}) parameter is enough to extract the complex permittivity. Normally, NRW technique requires these two parameters both for the extraction. If one of the reflection or transmission parameter is weak on measurement of the sample, N-R extraction technique should be selected [45, 49]. The transmission parameter S_{21} needs to be redefined for N-R technique as seen on Eq. 15 [21].

$$S_{21} = \frac{T(1 - \Gamma^2)}{1 - T^2\Gamma^2} \tag{15}$$

Transmission (T) and Reflection (Γ) coefficients are expressing interaction between material and electromagnetic wave. If the transmission (S_{21}) parameter seen on Eq. 15 is revised for the N-R technique, real (i) and imaginary (r) parts of complex permittivity are obtained as seen on Eq. 16 and 17, respectively. Measured parameter is indexed by (m). Tolerance value is obtained by taking the derivatives of Eq. 16 and 17 as seen on Eq. 18.

$$\varphi(\varepsilon_r, \varepsilon_i) = S_{21\_r}(\varepsilon_r, \varepsilon_i) - S_{21m\_r} \tag{16}$$

$$\phi(\varepsilon_r, \varepsilon_i) = S_{21\_i}(\varepsilon_r, \varepsilon_i) - S_{21m\_i} \tag{17}$$

$$D = \begin{vmatrix} \left(\dfrac{dS_{21\_r}}{d\varepsilon_r}\right) & \left(\dfrac{dS_{21\_r}}{d\varepsilon_i}\right) \\ \left(\dfrac{dS_{21\_i}}{d\varepsilon_r}\right) & \left(\dfrac{dS_{21\_i}}{d\varepsilon_i}\right) \end{vmatrix} \tag{18}$$

And next unknown values of ε_r and ε_i can be calculated by Eq. 19 and 20, where h and k are correction for the results, and o is initial value. The iteration is repeated until the desired value is obtained in this technique.

$$\varepsilon_r = \varepsilon_{r\_0} + h \tag{19}$$

$$\varepsilon_i = \varepsilon_{i\_0} + k \tag{20}$$

4.4. Comparison of analytical and numerical techniques

It is observed that the studies using NRW technique have different algorithms. Therefore, before the comparison, it is needed to have a decision which NRW algorithm will be compared with N-R. In this study, five different NRW algorithms, which are named as NRW1, NRW2, NRW3, NRW4 and NRW5, were evaluated.

According to NRW1, cut-off wavelength (λ_c) and the cut-off frequency (f_c) are used to obtain the complex permittivity (ε) by using Eq. 21. According to NRW2, the V_1 and V_2 values are represented sum and gap of S parameters as seen on Eq. 22 and 23, and impedance (Z) can be calculated by these values as seen on Eq. 24.

$$\lambda_{og} = \frac{1}{\sqrt{\dfrac{1}{\lambda_0^2} - \dfrac{1}{\lambda_c^2}}} \tag{21}$$

$$V_1 = S_{21} + S_{11} \tag{22}$$

$$V_2 = S_{21} - S_{11} \tag{23}$$

$$Z = \frac{\sqrt{1 + V_1}\sqrt{1 - V_2}}{\sqrt{1 - V_1}\sqrt{1 + V_2}} \tag{24}$$

The use of S-parameters in terms of voltage sum and difference is also seen in the NRW3 algorithm. X and transmission coefficient T are calculated as seen on Eq. 25 and 26, respectively, instead of calculating impedance (Z) value.

$$X = \frac{1 - V_1 V_2}{V_1 - V_2} \tag{25}$$

$$T = \frac{V_1 - \Gamma}{1 - V_1 \Gamma} \tag{26}$$

As seen in Eq. 26, transmission coefficient T is calculated, which is different to Eq. 10. In NRW4 algorithm, impedance (Z) value is calculated by using transmission (S_{11}) and reflection (S_{21}) parameters directly as seen on Eq. 27.

$$Z = \frac{(S_{11} + 1)^2 - S_{21}^2}{(S_{11} - 1)^2 - S_{21}^2} \tag{27}$$

In NRW5, impedance (Z) value that had been calculated by a different method is used to find the transmission coefficient T as seen on Eq. 28, which is not equal to Eq. 10 and 26.

$$T = \frac{S_{21}(Z + 1)}{(1 - S_{11})(Z - 1)} \tag{28}$$

As seen on these comparisons between NRW algorithms, it can be modeled with different approaches and used in material characterization. Although NRW cannot be used in the analysis of very thick materials, it is needed to demonstrate the accuracy of another technique incase used for analysis. Therefore, many studies have been compared with NRW in the literature.

The differences in NRW extraction technique (such as NRW1, NRW2, and NRW5) may also be applied to other extraction techniques. To prove this, the NRW algorithms were compared with the Newton-Raphson (N-R) results in the same way as seen above. The real and imaginary parts
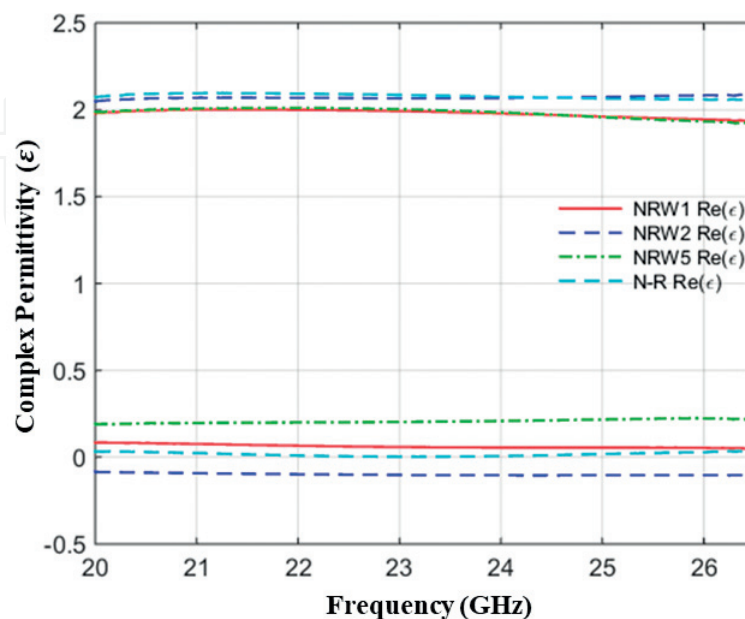

Figure 12. Comparison of Newton-Raphson and NRW techniques.

of the complex permittivity were examined. The results of the best performing algorithms (NRWs and N-R) are shown at the frequency band of 20–26.5 GHz on a thickness of 2 mm Teflon sample as seen in **Figure 12** [53]. According to results, the approaches of NRW3 and NRW5 are one-to-one overlap, and therefore, the results of NRW3 were removed from the **Figure 12**.

5. Comparison of FSM and MLD-TDS measurement methods

When the literature is reviewed, generally the dielectric properties of materials are analyzed with TDS in THz frequency region above 100 GHz. In recent years, using frequencies with FSM method are increased up to 500 GHz. Obtained results by the FSM method are compared to THz-TDS in the frequency down conversion methods by some researches. In this study, the results of FSM were compared with MLD-TDS system, which is cheaper than THz-TDS method. Two different measurement methods (FSM and MLD-TDS) were compared for different materials of various thicknesses, and necessary calculations were analyzed.

The results of complex permittivity of four samples are seen in **Figure 13**. As seen on the results, the values are close to each other except for a little gap. Although the systems are different, produced THz pulses will have same frequency. But it is noticed that not only operating in different medium but also the differences of extraction techniques affect the results.

These methods are preferred by various applications because of noncontact and nondestructive measurement possibilities, even they have different working principles. Before having a decision, which method is better, the subjects mentioned in **Table 3** and the measurement results should be considered as well.

The FSM method is disadvantageous to TDS because it requires a very expensive device such as the Vector Network Analyzer (VNA). In TDS method, cheaper laser diodes are used instead of expensive laser sources. FSM setup is simpler, because of having fewer components, and installation and testing measurement accuracy of TDS system take longer time. But performing broadband measurement with TDS is possible at one time contrary to FSM.

Due to antenna designs and productions are classified according to specific wave lengths, more than one antenna set is needed for wide band measurement or the measurement must be limited in a certain frequency band. For this reason, the discrete measurement is a limitation for FSM method.

FSM is advantageous when measuring length is concerned. Once the calibration process has been completed, the transmitted and reflected signals can be measured within seconds. But it is not possible for TDS. Only one w/o sample measurement takes 15 minutes. Though some displacement slider designs, which can measure 60 times per second, is pushed on the market to recover this, the price is needed to consider.

The stability of TDS method is adversely affected by the large number of components in the system. In addition, even if the system is protected in a housing, micron size displacement over time can cause to change laser beam path. In this case, the accuracy of measurement cannot be survived. From time to time, calibration or re-installation of measurement system may be
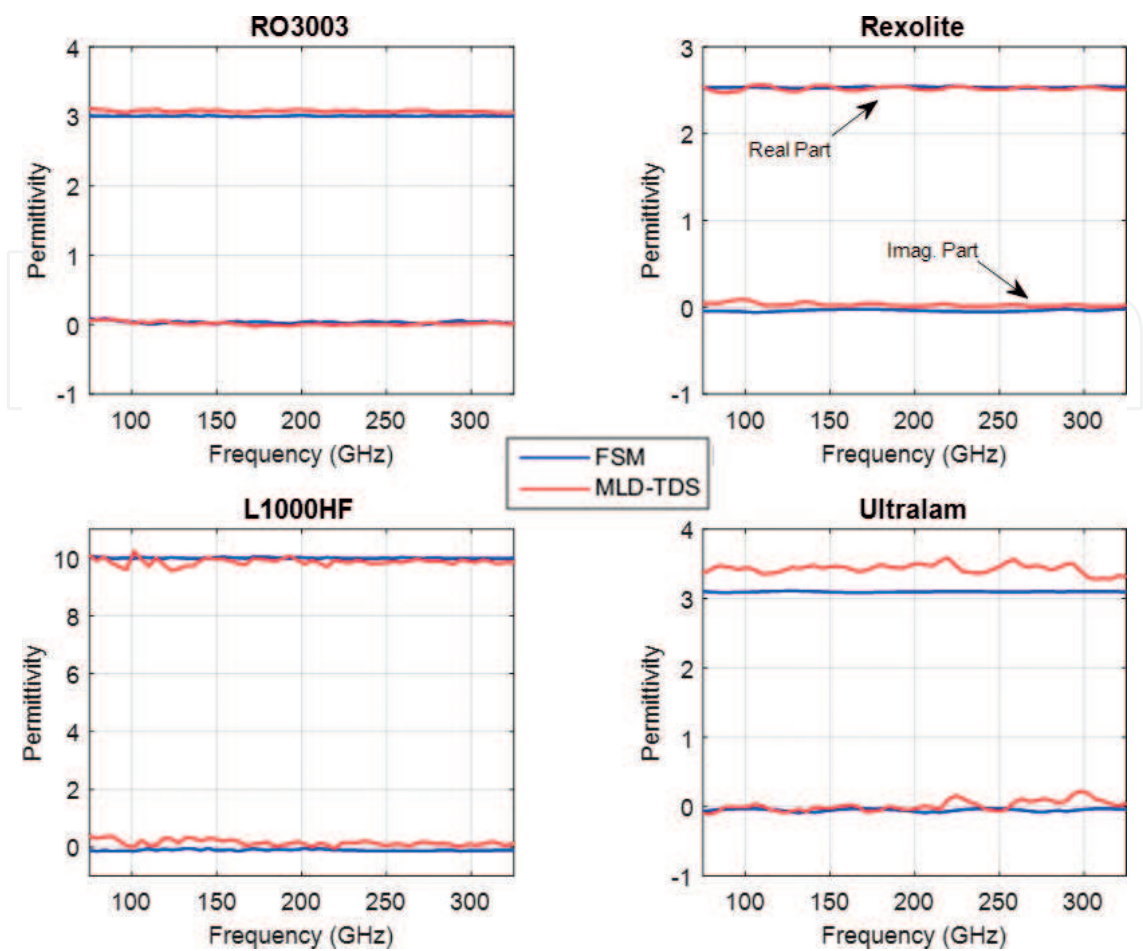
Figure 13. Comparison of complex permittivity with two different systems.

	FSM	MLD-TDS
Measurement frequency	Discrete	Wide
Installation length	Short	Long
Measurement length	Short	Long
Calculation length	Long	Long
System devices	Few	Many
Stability	Good	Not bad
Sensitivity	Good	Medium
Cost	Expensive	Cheap

Table 3. Comparison of FSM and MLD-TDS methods.

needed. In FSM method, even if there is any adjustment malfunction, the measurement can be continued by performing the calibration in a short time.

Comparisons made in this study are important in confirming that the results are obtained by using FSM method recently in THz frequency domain measurements. Although the

bandwidth is narrow, FSM has a good spectral resolution and dynamic range around 0.3 THz. The real parts of the complex permittivity values obtained by both methods are overlapped, but the results of the TDS system are better for the imaginary parts, probably because of multiple reflections effect in FSM. In TDS, measurements below 100 GHz, which are already outside the THz frequency domain, are not within the desired range due to the poor signal-to-noise ratio, and they are generally not shared. The measurement methods both have advantages in certain directions, and so they may be selected to use up to needs and priorities of the measurement will be done. FSM can provide more accurate results for the measurements in a certain frequency range, but TDS system can be offered for a wider frequency range as most efficient solution. These methods of measurement, thanks to developing technology, are being optimized for medical, biology, food, security, military, and other subjects to offer solutions to the problems.

6. Conclusion

In this chapter, measurement methods and extraction techniques used in material characterization are examined, and new materials were measured to show the accuracy and contribution of the proposed extraction techniques. The results of two different measurement methods with advantages relative to each other were compared, and approximate values were obtained as well as previously published studies. Thus, the usability of the FSM method in the THz frequency range has been shown using the results. Despite some disadvantages, TDS system, which uses the MLD as a light source, is more preferable than the FSM because it has a broadband spectrum measurement capability.

S-parameters collected during material measurement process were used to extract the dielectric properties with various extraction techniques, and successful results were obtained. By using Nicolson-Ross-Weir (NRW) method, which is the most basic calculation technique, various algorithms are compared and the Newton-Raphson approach which is the numerical analysis method is verified.

It must be provided that the generated THz signal is collimated to interact well with the material. In this context, the parabolic mirror, which is an optical component, can be preferred in order to efficiently use the FSM method in the THz frequency range. Due to the optical component used in the measurement method, the new system is called optical-like FSM. Due to the advantage of this system, hybrid systems consisting of optical and microwave measurement methods in the frequency range of 0.5–1 THz are predicted to be used more widely in the future.

Acknowledgements

Author details

Turgut Ozturk[1]* and Muhammet Tahir Güneşer[2]

*Address all correspondence to: turgutozturk@karabuk.edu.tr

1 Department of Electrical-Electronics Engineering, Karabuk University, Turkey

2 Department of Electrical-Electronics Engineering, Bursa Technical University, Turkey

References

[1] Skocik P, Neumann P. Measurement of complex permittivity in free space. Procedia Engineering. 2015;**100**:100-104. DOI: 10.1016/j.proeng.2015.01.347

[2] Rajesh Mohan RM, Mridula S, Mohanan P. Study and analysis of dielectric behavior of fertilized soil at microwave frequency. EJAET. 2015;**2**:73-79

[3] Nelson SO. Measurement of microwave dielectric properties of particulate materials. Journal of Food Engineering. 1994;**21**:365-384. DOI: 10.1016/0260-8774(94)90080-9

[4] Rocha LS, Junqueira CC, Gambin E, Nata Vicente A, Culhaoglu AE, Kemptner E. A free space measurement approach for dielectric material characterization. In: SBMO/IEEE MTT-S International Microwave and Optoelectronics Conference. IEEE; 2013. pp. 1-5. DOI: 10.1109/IMOC.2013.6646474

[5] Tereshchenko OV, Buesink FJK, Leferink FBJ. An overview of the techniques for measuring the dielectric properties of materials. In: XXXth URSI General Assembly and Scientific Symposium. IEEE; 2011. pp. 1-4. DOI: 10.1109/URSIGASS.2011.6050287

[6] Jilani MT, Zaka M, Khan AM, Khan MT, Ali SM. A brief review of measuring techniques for characterization of dielectric materials. International Journal of Information Technology and Electrical Engineering. 2012;**1**:1-5

[7] Ghodgaonkar DK, Varadan VV, Varadan VK. Free-space measurement of complex permittivity and complex permeability of magnetic materials at microwave frequencies. IEEE Transactions on Instrumentation and Measurement. 1990;**39**:387-394. DOI: 10.1109/19.52520

[8] Petersson LER, Smith GS. An estimate of the error caused by the plane-wave approximation in free-space dielectric measurement systems. IEEE Transactions on Antennas and Propagation. 2002;**50**:878-887. DOI: 10.1109/TAP.2002.1017671

[9] Ozturk T, Morikawa O, Ünal İ, Uluer İ. Comparison of free space measurement using a vector network Analyzer and low-cost-type THz-TDS measurement methods between 75 and 325 GHz. Journal of Infrared, Millimeter, and Terahertz Waves. 2017;**38**:1241-1251. DOI: 10.1007/s10762-017-0410-1

[10] Scheller M, Koch M. Terahertz quasi time domain spectroscopy. Optics Express. 2009;**17**: 17723. DOI: 10.1364/OE.17.017723

[11] Morikawa O, Tonouchi M, Hangyo M. Sub-THz spectroscopic system using a multimode laser diode and photoconductive antenna. Applied Physics Letters. 1999;**75**:3772. DOI: 10.1063/1.125451

[12] Ozturk T, Hudlička M, Uluer İ. Development of measurement and extraction technique of complex permittivity using transmission parameter S21 for Millimeter wave frequencies. Journal of Infrared, Millimeter, and Terahertz Waves. 2017;**38**:1510-1520. DOI: 10.1007/s10762-017-0421-y

[13] Ozturk T, Elhawil A, Uluer İ, Tahir M. Development of extraction techniques for dielectric constant from free-space measured S-parameters between 50 and 170 GHz. Journal of Materials Science: Materials in Electronics. 2017:1-7. DOI: 10.1007/s10854-017-6953-z

[14] Narayan RM, Vu KT. Free-space microwave measurement of low moisture content in powdered foods. Journal of Food Processing & Preservation. 2000;**24**:39-56. DOI: 10.1111/j.1745-4549.2000.tb00404.x

[15] Kim KB, Park SG, Kim JY, Kim JH, Lee CJ, Kim MS, et al. Measurement of moisture content in powdered food using microwave free-space transmission technique. Key Engineering Materials. 2006;**321**:1196-1200. DOI: 10.4028/www.scientific.net/KEM.321-323.1196

[16] Kraszewski A, Trabelsi S, Nelson S. Comparison of density-independent expressions for moisture content determination in wheat at microwave frequencies. Journal of Agricultural Engineering Research. 1998;**71**:227-237. DOI: 10.1006/jaer.1998.0320

[17] Mohan RR, Paul B, Mridula S, Mohanan P. Measurement of soil moisture content at microwave frequencies. Procedia Computer Science. 2015;**46**:1238-1245. DOI: 10.1016/j.procs.2015.01.040

[18] Wee FH, Soh PJ, Suhaizal AH, Nornikman H, Ezanuddin AA. Free space measurement technique on dielectric properties of agricultural residues at microwave frequencies. In: International Microwave and Optoelectronics Conference. IEEE; 2009. pp. 183-187. DOI: 10.1109/IMOC.2009.5427603

[19] Chen LF, Ong CK, Neo CP, Varadan VV, Varadan VK. Microwave Electronics. 1st ed. Chichester, UK: John Wiley & Sons, Ltd; 2004. DOI: 10.1002/0470020466

[20] Al-Mously SIY. A modified complex permittivity measurement technique at microwave frequency. International Journal of New Computer Architectures and Their Applications. 2012;**2**:389-401

[21] Puthukodan S, Dadrasnia E, Vinod VKT, Lamela Rivera H, Ducournau G, Lampin J-F. Optical properties of carbon nanotube thin films in subterahertz frequency regime. Microwave and Optical Technology Letters. 2014;**56**:1895-1898. DOI: 10.1002/mop.28477

[22] Kazemipour A, Hudlicka M, Yee S-K, Salhi MA, Allal D, Kleine-Ostmann T, et al. Design and calibration of a compact quasi-optical system for material characterization in Millimeter/Submillimeter wave domain. IEEE Transactions on Instrumentation and Measurement. 2015;**64**:1438-1445. DOI: 10.1109/TIM.2014.2376115

[23] Akhtar MJ, Spiliotis NG, Omar AS. An experimental setup for the microwave imaging of inhomogeneous dielectric bodies. In: IEEE Antennas and Propagation Society International Symposium. IEEE; 2004. pp. 225-228. DOI: 10.1109/APS.2004.1329607

[24] Ozturk T, Uluer İ, Ünal İ. Materials classification by partial least squares using S-parameters. Journal of Materials Science: Materials in Electronics. 2016;**27**:12701-12706. DOI: 10.1007/s10854-016-5404-6

[25] Zhang J, Nakhkash M, Huang Y. Electromagnetic imaging of layered building materials. Measurement Science and Technology. 2001;**12**:1147-1152. DOI: 10.1088/0957-0233/12/8/322

[26] Friedsam GL, Biebl EM. A broadband free-space dielectric properties measurement system at millimeter wavelengths. In: 20th Bienn. Conf. Precis. Electromagn. Meas. IEEE; 1997. pp. 210-211. DOI: 10.1109/CPEM.1996.546779

[27] Yin H-C, Chao Z-M, Xu Y-P. A new free-space method for measurement of electromagnetic parameters of biaxial materials at microwave frequencies. Microwave and Optical Technology Letters. 2005;**46**:72-78. DOI: 10.1002/mop.20905

[28] Ghodgaonkar DK, Varadan VV, Varadan VK. A free-space method for measurement of dielectric constants and loss tangents at microwave frequencies. IEEE Transactions on Instrumentation and Measurement. 1989;**38**:789-793. DOI: 10.1109/19.32194

[29] Grignon R, Afsar MN, Wang Y, Butt S. Microwave broadband free-space complex dielectric permittivity measurements on low loss solids. In: 20th IEEE Instrumentation Technology Conference. IEEE; 2003. pp. 865-870. DOI: 10.1109/IMTC.2003.1208278

[30] Ajami A, Akkara-Aketalin T, Shakhtour H, Heberling D. Experimental investigations of accuracy improvement and limitations of a free space measurement system including thin lenses. In: 7th European Conference on Antennas and Propagation. 2013. pp. 4064-4067

[31] Scheller M, Koch M. Multi-mode continuous wave terahertz systems-quasi time domain spectroscopy. Conference on Lasers Electro-Optics. 2010;**1**:2-3

[32] Scheller M, Dürrschmidt SF, Stecher M, Koch M. Terahertz quasi-time-domain spectroscopy imaging. Applied Optics. 2011;**50**:1884. DOI: 10.1364/AO.50.001884

[33] Hangyo M. Development and versatile applications of terahertz time-domain spectroscopy. In: 39th International Conference on Infrared, Millimeter, Terahertz Waves. IEEE; 2014. pp. 1-4. DOI: 10.1109/IRMMW-THz.2014.6955988

[34] Tani M, Morikawa O, Matsuura S, Hangyo M. Generation of terahertz radiation by photomixing with dual- and multiple-mode lasers. Semiconductor Science and Technology. 2005;**20**:S151-S163. DOI: 10.1088/0268-1242/20/7/005

[35] Morikawa O, Fujita M, Takano K, Hangyo M. Sub-terahertz spectroscopic system using a continuous-wave broad-area laser diode and a spatial filter. Journal of Applied Physics. 2011;**110**:063107. DOI: 10.1063/1.3639296

[36] Tani M, Matsuura S, Sakai K, Hangyo M. Multiple-frequency generation of sub-terahertz radiation by multimode LD excitation of photoconductive antenna. IEEE Microwave and Guided Wave Letters. 1997;**7**:282-284. DOI: 10.1109/75.622540

[37] Hyodo M, Tani M, Matsuura S, Onodera N, Sakai K. Generation of millimetre-wave radiation using a dual-longitudinal-mode microchip laser. Electronics Letters. 1996;**32**: 1589. DOI: 10.1049/el:19961041

[38] Morikawa O, Tonouchi M, Tani M, Sakai K, Hangyo M. Sub-THz emission properties of photoconductive antennas excited with multimode laser diode. Japanese Journal of Applied Physics. 1999;**38**:1388-1389. DOI: 10.1143/JJAP.38.1388

[39] Zhang X-C, Xu J. Introduction to THzWave Photonics; 2010

[40] Rolfes I, Schiek B. Calibration methods for microwave free space measurements. Advances in Radio Science. 2005;**2**:19-25. DOI: 10.5194/ars-2-19-2004

[41] Bartley PG, Begley SB. A new free-space calibration technique for materials measurement. In: IEEE International Instrumentation and Measurement Technology Conference. IEEE; 2012. pp. 47-51. DOI: 10.1109/I2MTC.2012.6229351

[42] Will B, Rolfes I. Application of the thru-network-line self-calibration method for free space material characterizations. In: Proceedings of 2012 International Conference on Electromagnetic Advanced Applications. ICEAA'12. 2012. pp. 831-834. DOI: 10.1109/ICEAA.2012.6328749

[43] Nicolson AM, Ross GF. Measurement of the intrinsic properties of materials by time-domain techniques. IEEE Transactions on Instrumentation and Measurement. 1970;**19**: 377-382. DOI: 10.1109/TIM.1970.4313932

[44] Weir WB. Automatic measurement of complex dielectric constant and permeability at microwave frequencies. Proceedings of the IEEE. 1974;**62**:33-36. DOI: 10.1109/PROC.1974.9382

[45] Elhawil A, Vounckx R, Zhang L, Koers G, Stiens J. Comparison between two optimisation algorithms to compute the complex permittivity of dielectric multilayer structures using a free-space quasi-optical method in W-band. IET Science, Measurement and Technology. 2009;**3**:13-21. DOI: 10.1049/iet-smt:20070085

[46] Liang C, Li L, Zhai H. Low-cost free-space measurement of dielectric constant at Ka band. IEE Proceedings: Microwaves, Antennas and Propagation. 2004;**151**:271-276. DOI: 10.1049/ip-map

[47] Jurado A, Escot D, Poyatos D, Montiel I. Application of artificial neural networks to complex dielectric constant estimation from free-space measurements. In: Methods Model. Artif. Nat. Comput. 2009. pp. 517-526. DOI: 10.1007/978-3-642-02264-7_53

[48] Zivkovic I, Murk A. Extraction of dielectric and magnetic properties of carbonyl iron powder composites at high frequencies. Journal of Applied Physics. 2012;**111**. DOI: 10.1063/1.4725473

[49] Elhawil A, Koers G, Zhang L, Stiens J, Vounckx R. Reliable method for material characterisation using quasi-optical free-space measurement in W-band. IET Science, Measurement and Technology. 2009;**3**:39-50. DOI: 10.1049/iet-smt:20070086

[50] Gagnon N, Shaker J, Berini P, Roy L, Petosa A. Correction and extraction techniques for dielectric constant determination using a Ka-band free-space measurement system. In: 32nd European Microwave Conference 2002. IEEE; 2002. pp. 1-4. DOI: 10.1109/EUMA.2002.339410

[51] Baker-Jarvis J, Jones C, Riddle B, Janezic M, Geyer RG, Grosvenor JH, et al. Dielectric and magnetic measurements: A survey of nondestructive, quasi-nondestructive, and process-control techniques. Research in Nondestructive Evaluation. 1995;**7**:117-136. DOI: 10.1007/BF02538826

[52] Rutpralom T, Chamnongthai K, Kumhom P, Krairiksh M. Nondestructive durian maturity determination by using microwave free space measurement. In: IEEE International Symposium on Circuits & Systems. IEEE; 2006. pp. 1351-1354. DOI: 10.1109/ISCAS.2006.1692844

[53] Ozturk T, Elhawil A, Düğenci M, Ünal İ, Uluer İ. Extracting the dielectric constant of materials using ABC-based ANNs and NRW algorithms. Journal of Electromagnetic Waves and Applications. 2016;**30**:1785-1799. DOI: 10.1080/09205071.2016.1215266